Electronic Supplementary Information for:

Evaluation of Brønsted and Lewis acid sites in H-ZSM-5 and H-USY with or without metal modification using probe molecule-synchrotron X-ray powder diffraction

Benedict T.W. Lo,[a,b] Wei-che Lin,[a] Molly Meng Jung Li,[a,b] Sarah Day,[c] Chiu Tang,[c] Shik Chi Edman Tsang[a*]

[a] Wolfson Catalysis Centre, University of Oxford, Oxford, OX1 3QR, UK

[b] Hong Kong Polytechnic University, Hong Kong, China

[c] Diamond Light Source Ltd, Harwell Science and Innovation, Didcot, OX11 0DE, UK

This PDF file includes:

1. Materials and Methods

Materials

H-ZSM-5

High-quality H-USY and H-ZSM-5 samples are commercially available. The structural properties of H-USY (***FAU***, Si/Al = 7.3, from TOSOH) and H-ZSM-5 (***MFI***, Si/Al = 18.5, from SRIPT-SINOPEC) zeolites and their respective structural properties were previously reported (see Figure S1 in the Supporting Information for the microscopy images)[1,2]. High-quality commercial H-ZSM-5 and H-USY samples were supplied by SRIFT-Sinopec, China. The H-ZSM-5 (SiO_2:Al_2O_3 = 1:38.5), containing one Al (i.e., one Brønsted acid site) per asymmetric unit, with the space group of *Pnma* was deliberately chosen. The Al substituted site has been determined specifically at the framework T6 site with the Brønsted acid site located at O18 in our previous work (via loading zeolites with base probe molecules; the zeolite samples were measured with high-resolution synchrotron X-ray powder diffraction (SXRD) using the high-precision multi-analyser crystal detectors).[1] The BET surface area is 330 m^2 g^{-1}. Attempts were also made to establish H-ZSM-5 with higher Al/Si ratios than the above commercial H-ZSM-5 material. However, it was unfortunate that there were either high levels of impurities or much lesser crystallinity than this H-ZSM-5 sample containing only 1 Al in each asymmetric segment in a unit cell (SiO_2:Al_2O_3 = 38.5). As a result, the Rietveld refinements of the corresponding samples were not satisfactory.

Ag-ZSM-5 and Zn-ZSM-5

Modified H-ZSM-5 with different metal ions were prepared by aqueous ion-exchange of H-ZSM-5 with $AgNO_3$ and $Zn(NO_3)_2$ solutions. The ion-exchange was carried at ambient temperature by mixing 1.0 g H-ZSM-5 with 30 mL aqueous solution which contains an equivalent of one metal ion per unit cell of H-ZSM-5 for 5 h. Then, the samples were rinsed five times with deionized water and dried at 70 °C overnight. In addition, the BET surface area of Ag/ZSM-5 and Zn/ZSM-5 is 336 and 334 m^2 g^{-1} respectively (no apparent change in surface area as compared with the unmodified H-ZSM-5). Through ion-exchange of Ag^+ and Zn^{2+} with H-ZSM-5, Ag-ZSM-5 and Zn-ZSM-5 were prepared. To reduce migration of the metal sites, the samples were not calcined.

Methods

Synchrotron X-ray powder diffraction (SXRD) and Rietveld refinement

SXRD data were collected at Beamline I11, Diamond Light Source, Harwell, UK.[3] The energy of the incident X-ray flux was set at 15 keV. The wavelength and the 2θ-zero point were refined using a diffraction pattern obtained from a high-quality silicon powder (SRM640c). High-resolution SXRD data were obtained from the zeolite samples using the multi-analyzer crystals (MAC) detectors. The patterns were collected in the 2θ range 0-150° with 0.001° data binning. Each MAC pattern was collected for an hour for good statistics. In total, there are 4190 hkl reflections measured (within the region of refinement (2θ = 3-55°)). From a mathematical perspective, the number of variables should not exceed the number of observables. In the Rietveld refinements performed in this work, the number of structural parameters has not exceeded 190.

Using the TOPAS software, the lattice parameters were refined using the Le Bail method, and the Rietveld refinement analyses of the diffraction patterns were performed. The starting coordinates used were based on the H-ZSM-5 zeolite model by Heo *et al.* for sample refinement.[4] The background curve was fitted by a Chebyshev polynomial with 20 coefficients. The Thompson-Cox-Hastings pseudo-Voigt peak function proposed by Thompson *et al.* was applied.[5] The scale factor and lattice parameters were allowed to vary for all the histograms.

The final refined structural parameters for each data histogram were carried out using the Rietveld method with the fractional coordinates (*x, y, z*) and isotropic displacement factors (B_{eq}) for all atoms. In addition, the quality of fit was assessed by the R_{wp} and *gof* values ($gof = R_{wp}/R_{exp}$), where R_{exp} represents the quality of the data. So, the R_{wp} value should be close to R_{exp} for a good fit.

(i) Framework atoms

In principle, upon organic molecule adsorption, the positions of the framework atoms may change slightly – a small deviation from the model by Heo *et al.* Therefore, prior the refinement of the entire structure with guest molecules, the framework atoms were first refined, to avoid a miscalculation of the structure that reaches the global minimum of the refinement by changing the entire framework. As the

guest molecules that were used do not consist of any heavy atoms, it is reasonable to assume the guest molecules only minimally contribute to the high 2θ angle reflections. Thus, the fractional coordinates and the B_{eq} values of the framework atoms (Si and O) were fixed and all other parameters were refined over the 2θ range of 30-55°.

(ii) Fourier analysis

Over the 2θ range of 3-55°, the Fourier analysis was used to identify the positions with the highest remaining electron density in the framework, once the positions of the framework atoms have been refined.

(iii) Inclusion of probe molecules

Based on the Fourier analysis, a Monte Carlo-based simulated annealing technique in which the probe molecules are treated as rigid bodies was used to locate their positions in the H-ZSM-5. The probe molecule rigid body Z-matrices were refined while keeping the fractional coordinates of the framework atoms fixed.

The H-ZSM-5 pre-adsorbed with furan/DMF sample were refined using three rigid body Z-matrices describing probe molecule at fixed bond distances and angles, it was first applied to be simulated annealed using the Rietveld method (while the fractional coordinates of the framework were fixed). The site occupancy factors (SOF) of one of the three rigid body Z-matrices approached zero. Thus, the simulated annealing technique ensures the correct number of probe molecule sites. The extra presence of the electron density in the centre of the void has been accounted by various 'dummy' atoms.

After identifying the number and location of the furan/DMF molecules, the SOF values were refined. Then, all the relevant parameters were all relaxed to be refined, by simulated annealing repeatedly for an hour to ensure the global minimum has been reached. In general, the global minimum is indicated by the lowest R_{wp} and *gof* values.

However, in some cases, the derived crystal structures did not make much chemical sense, e.g. the probe molecules are located far too close to the framework – this required a closer check of the parameters before repeating refinement procedure. Ultimately, several criteria were met to ensure the high quality

and reliability of the refinement, namely, (i) the global minimum has been reached, (ii) the derived crystal structure fits chemical sense, (iii) reasonable systematic error values for all the refined parameters, and (iv) reasonable SOF and B_{eq} values.

The B_{eq} were constrained in the following way: (i) all the T-sites (T = Al, Si) share the same value, and the values for the O-sites are twice the B_{eq} for the T-sites, and (ii) the B_{eq} of C and O atoms were all arbitrary fixed at 8 $Å_2$ for the room temperature measurements (298 K).[6–10] The crystallographic parameters are summarized in Tables S1-S4. The position errors of furan and DMF are estimated from the percentage errors of the translation and rotation axes of the rigid bodies.

Thermogravimetric analysis (TGA)

The TGA measurements of the ZSM-5 zeolite samples pre-adsorbed with DMF and furan were performed in air (100 cm_3 min_{-1}) up to 600 °C using TA Instruments SDT Q600 at 5 °C min_{-1}.

Solid-state nuclear magnetic resonance spectroscopy (ssNMR)

2.1 Electron microscopy

The transmission electron microscopy (TEM) images (see Fig. S1) clearly shows a uniform distribution of zeolite which has a mean particle size of *ca.* 2 μm x 1 μm x 1 μm. The uniform, micron particle size and high-quality crystallinity ensure an accurate and reliable Rietveld refinement of the corresponding SXRD data. From the inductive coupled plasma-atomic emission spectroscopy (ICP-AES) measurement, it was found that the Al:Si ratio is 1:38.5 which is very close to the synthesis ratio.

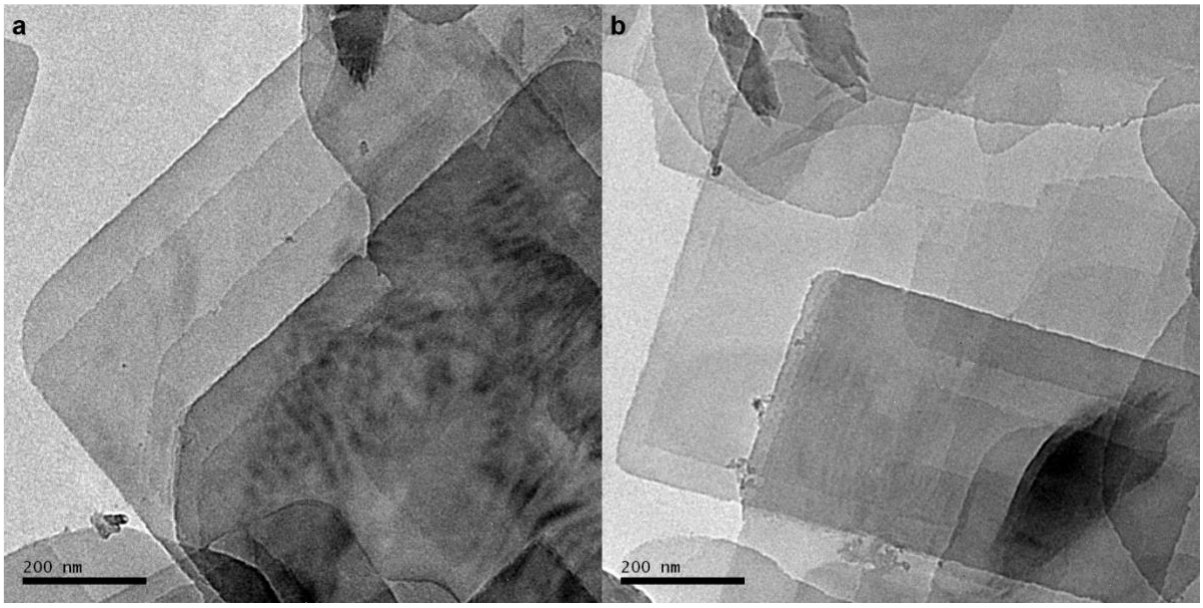

Figure S1. TEM images. Images showing the particle size (*ca.* 2 μm × 1 μm × 1 μm) (a) H-ZSM-5 and (b) Ag-ZSM-5, showing no observable nano-particles on the zeolite external surface.

2.2 Solid-state nuclear magnetic resonance spectroscopy

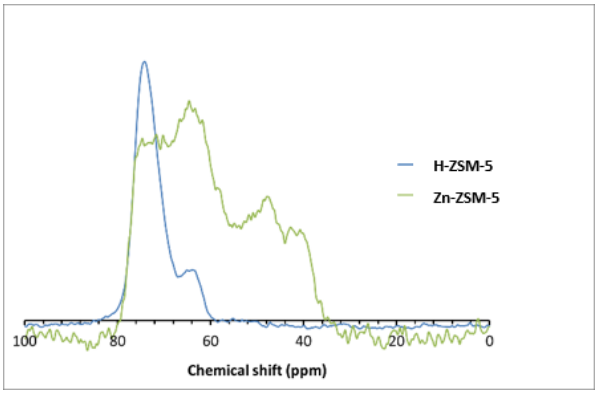

Figure S2. ^{31}P MAS NMR spectra of TMPO adsorbed on H-ZSM-5 and Zn-ZSM-5.

We further probed nuclear magnetic resonance spectroscopy (NMR) to measure the acidity before and after metal incorporation. Trimethylphosphine oxide (TMPO)-adsorbed sample was loaded for ^{31}P magic-angle-spinning (MAS) NMR measurements. The probe NMR spectra with TMPO of H-ZSM-5 and Zn-ZSM-5 are presented in Figure S2. Despite the poor-quality of the spectrum with the incorporation of Zn, some BASs (70 - 80 ppm) are retained after ion-exchange. The extra feature at lower chemical shifts can be ascribed to the interaction between the Lewis acidic species and the Lewis basic TMPO.[8] The relatively broad peaks are caused by the presence of more than one Zn sites (as suggested by the reviewer). The integrated area of TMPO molecule adsorbed (0.4 mmol g^{-1}) is consistent with the value from the structure refinement of the diffraction data. We note the difficulty in directly interpreting the strengths of the BASs and metal adsorption sites due to the core difference between the interaction with the probe molecules.

2.3 Thermogravimetric analysis

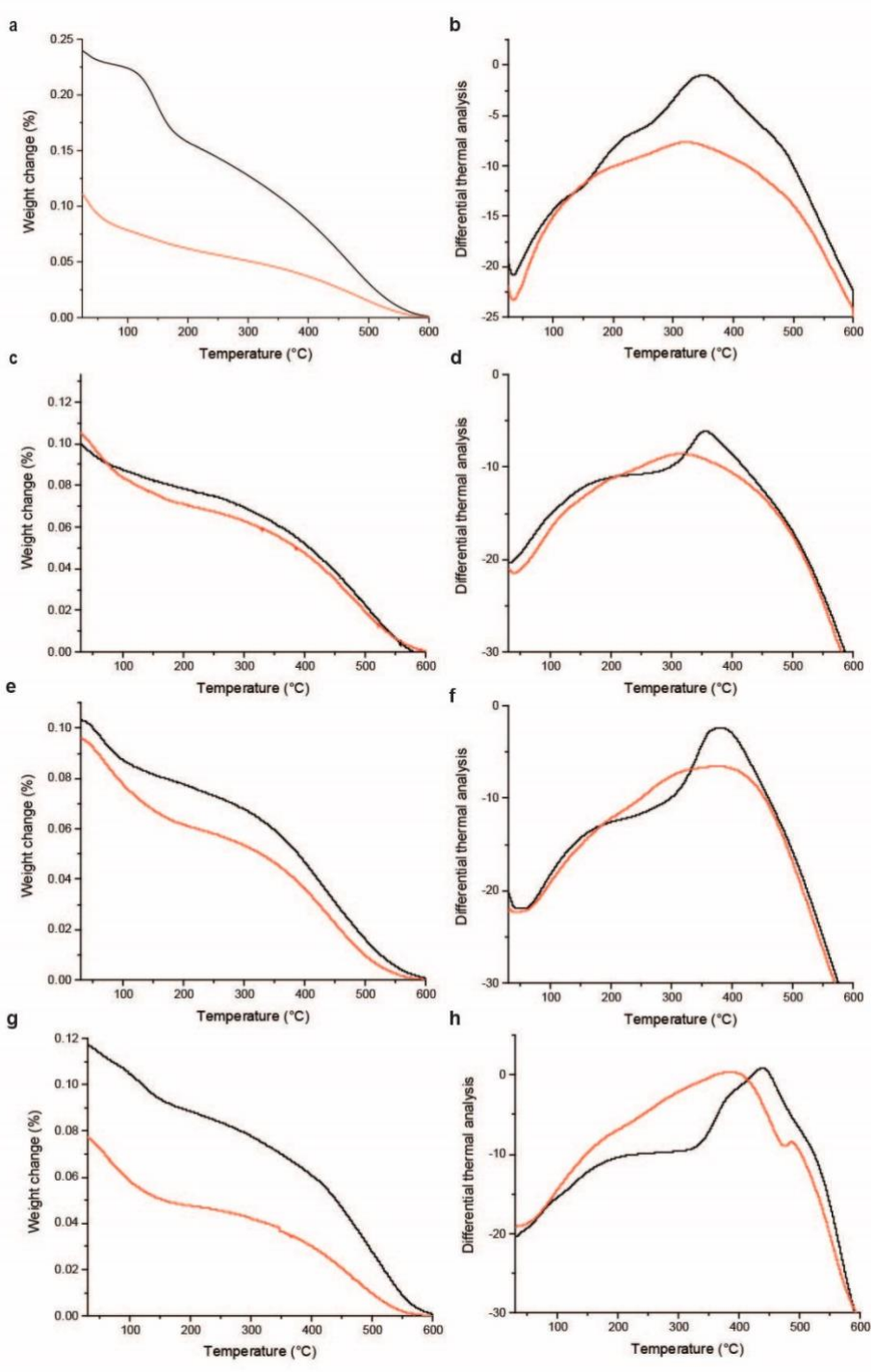

Figure S3. TGA and their corresponding differential profiles of (**a, b**) H-USY, (**c, d**) H-ZSM-5, (**e, f**) Ag-ZSM-5, and (**g, h**) Zn-ZSM-5. Red curve = furan, and black curve = DMF.

2.4 Crystallographic and atomic parameters

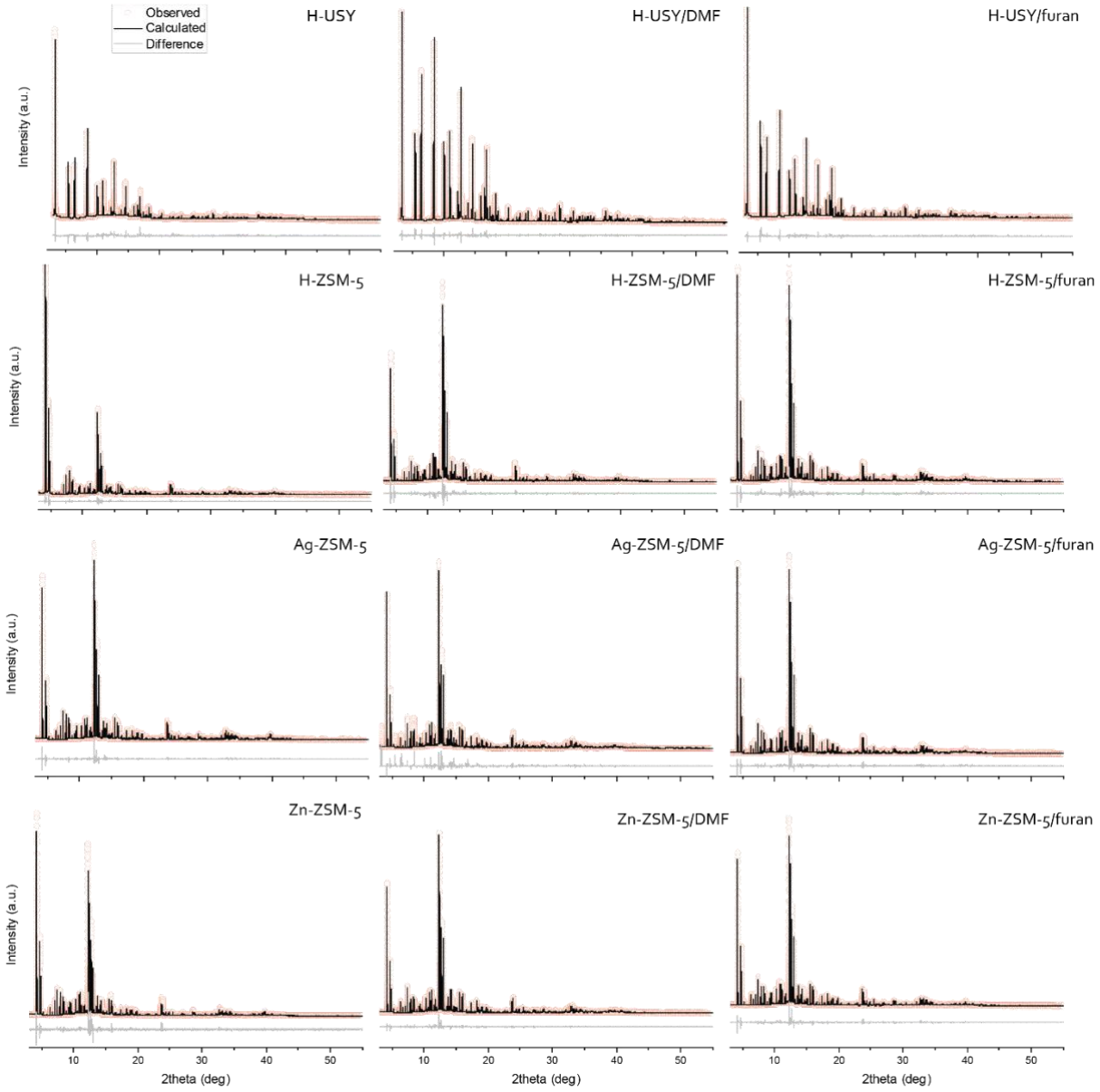

Figure S4. The SXRD patterns and Rietveld refinement profiles of DMF and furan independently pre-adsorbed on H-ZSM-5 and H-USY, and the Ag/Zn modified samples at 25 °C (pre-treated at 200 °C to remove physisorbed adsorbates). The SXRD patterns were measured at Diamond Light Source Beamline I11 using the multi-analyser crystals detector. The crystallographic parameters are summarised in Tables S3.

The verification of the accuracy of the Rietveld refinement processes is summarized in Tables S2-S3. The basic crystallographic parameters are summarized in Table S1 and the atomic parameters are summarized in Table S5.

As displayed in Table S2, by refining different numbers of DMF molecules for simulated annealing, the R_{wp} and gof become progressively lower when the first two DMF molecules are applied, as similar to our previous fittings but with more better fitting parameters. However, the third DMF molecule overlaps with the second DMF in both position and the fitting for DMF2 and DMF3 seem to split this regional electron density into relatively low occupancies. Therefore, the refinement with three DMF molecules is rejected but two DMF sites are taken to be closer to the genuine situation.

From repeatedly (an average of 10 times) manually placing the refined positions of the DMF1 site away from the framework, the derived O18-O_{DMF1} interatomic distances were still converged within the same range of ± 0.04 Å (with ±0.001 of R_{wp}). In addition to the repeated attempts, we have also further investigated the sensitivity of the R-factors versus a small change in the location of the adsorbed DMF sites. It can be seen from Table S3(a) and Table S3(b) that, a slight change in the rotational and translational axes (by ± 0.01 fractional unit) of the DMF1 site Z-matrix produces noticeable changes in the fitting R-factors. Through further simulated annealing, this DMF1 Z-matrix can clearly converge into the similar refined locations (± 0.002 in terms of fractional units) where the R-factors are the lowest. One concern was that such small changes might have taken the fitting away from local minimum. As a result, a larger change in the translational axes (by ± 0.2 fractional unit) of the DMF1 site Z-matrix has also been conducted (Table S3(c)) but the same converging points have been reached. To our best attempts, the reliability of the Rietveld refinement process and the determination of the locations of the DMF sites have been satisfactorily taken place over such revised fittings. This process has also been applied to all other zeolite samples.

Regarding the refinement of the Z-matrices for the complexes for M-DMF-$(H_2O)_3$, the initial rigid bodies have assumed the M-O bond distances of 2 Å, and the standard tetrahedral internal angles of 109.5° and dihedral angles of 120°. Meanwhile, the starting model has also assumed the DMF/furan molecule is perpendicular to the O_{H2O1} site.

Table S1(a). Summary of the crystallographic data of the SXRD measurements of H-ZSM-5 pre-adsorbed with DMF and furan.

Adsorbate species	Without	DMF	furan
Wavelength (Å) (synchrotron)	0.825900(1)	0.825251(1)	0.825251(1)
2θ - zero point (°)	-0.004944(1)	-0.00267(1)	-0.00267(1)
Space group	*Pnma*	*Pnma*	*Pnma*
Crystal system	Orthorhombic	Orthorhombic	Orthorhombic
a (Å)	20.12885(3)	20.11937(3)	20.10656(3)
b (Å)	19.95535(3)	19.94496(3)	19.95416(3)
c (Å)	13.43143(2)	13.41056(2)	13.42619(2)
V (Å$_3$)	5395.17(2)	5381.39(3)	5382.70(3)
2θ range for refinement (°)	3-55	3-55	3-55
Detector	Multi-analyser crystals	Multi-analyser crystals	Multi-analyser crystals
Number of parameters	148	160	160
Number of *hkl*s	4190	4190	4190
Refinement methods	Rietveld	Rietveld	Rietveld
$R_{wp}/R_{exp}/R_p$ (%)	6.688/4.135/5.332	8.336/3.339/6.410	8.757/3.104/6.611
gof	2.237	2.496	2.913

R_{wp}: weighted profile; R_{exp}: expected; R_p: profile; *gof:* goodness-of-fit.

Table S1(b). Summary of the crystallographic data of the SXRD measurements of Ag-ZSM-5 pre-adsorbed with DMF and furan.

Adsorbate species	Without	DMF	furan
Wavelength (Å) (synchrotron)	0.825771(1)	0.825850(1)	0.825850(1)
2θ - zero point (°)	-0.001932(1)	0.010275(1)	0.010275(1)
Space group	*Pnma*	*Pnma*	*Pnma*
Crystal system	Orthorhombic	Orthorhombic	Orthorhombic
a (Å)	20.13675(3)	20.16619(3)	20.11668(3)
b (Å)	19.95928(3)	19.97678(3)	19.93287(3)
c (Å)	13.43725(2)	13.45291(2)	13.42730(2)
V (Å$_3$)	5400.63(3)	5419.58(3)	5384.12(3)
2θ range for refinement (°)	3-55	3-55	3-55
Detector	Multi-analyser crystals	Multi-analyser crystals	Multi-analyser crystals
Number of parameters	138	152	152
Number of *hkl*s	4190	4190	4190
Refinement methods	Rietveld	Rietveld	Rietveld
$R_{wp}/R_{exp}/R_p$ (%)	11.277/8.447/8.707	6.555/2.955/4.974	7.674/2.757/5.924
gof	1.335	2.218	2.784

Table S1(c). Summary of the crystallographic data of the SXRD measurements of Zn-ZSM-5 pre-adsorbed with DMF and furan.

Adsorbate species	Without	DMF	furan
Wavelength (Å) (synchrotron)	0.825900(1)	0.825251(1)	0.825251(1)
2θ - zero point (°)	-0.004944(1)	-0.00267(1)	-0.00267(1)
Space group	*Pnma*	*Pnma*	*Pnma*
Crystal system	Orthorhombic	Orthorhombic	Orthorhombic
a (Å)	20.12885(3)	20.10656(3)	20.11937(3)
b (Å)	19.95555(3)	19.95416(3)	19.94496(3)
c (Å)	13.43143(3)	13.41619(2)	13.41056(2)
V (Å$_3$)	5395.172(27)	5382.70(2)	5381.39(2)
2θ range for refinement (°)	3-55	3-55	3-55
Detector	Multi-analyser crystals	Multi-analyser crystals	Multi-analyser crystals
Number of parameters	146	160	160
Number of *hkl*s	4190	4190	4190
Refinement methods	Rietveld	Rietveld	Rietveld
$R_{wp}/R_{exp}/R_p$ (%)	7.896/3.529/6.086	9.994/2.958/7.355	7.772/2.819/5.858
gof	2.237	3.378	2.757

Table S1(d). Summary of the crystallographic data of the SXRD measurements of H-USY pre-adsorbed with DMF and furan.

Adsorbate species	Without	DMF	furan
Wavelength (Å) (synchrotron)	0.825932(1)	0.825258(1)	0.825258(1)
2θ - zero point (°)	-0.00506(1)	-0.00271(1)	-0.00271(1)
Space group	*Fd-3m*	*Fd-3m*	*Fd-3m*
Crystal system	Cubic	Cubic	Cubic
a (Å)	24.36653(4)	24.38459(4)	24.38632(4)
V (Å$_3$)	14489.705(74)	14499.280(76)	14502.364(73)
2θ range for refinement (°)	3-55	3-55	3-55
Detector	Multi-analyser crystals	Multi-analyser crystals	Multi-analyser crystals
Number of parameters	34	48	48
Number of *hkl*s	563	563	563
Refinement methods	Rietveld	Rietveld	Rietveld
$R_{wp}/R_{exp}/R_p$ (%)	8.916/3.474/6.879	8.617/2.624/6.174	8.989/2.787/6.290
gof	2.567	3.283	3.226

Table S2. Rietveld fitting attempts that verifies the number of DMF sites in H-ZSM-5.

Fitting attempts with different number of DMF sites	**Rietveld** R_{wp} / R_{exp} /R_p / *gof*
H-ZSM-5· 0DMF	23.082/3.343/16.382/6.904
H-ZSM-5· 1DMF	15.087/3.343/10.624/4.513
H-ZSM-5· 2DMF	8.336/3.339/6.379/2.487
H-ZSM-5· 3DMF	8.254/3.339/6.338/2.469

Table S3(a). Impact on the R-factors over a manual change in the rotational axes of the DMF1 site Z-matrix (without further minimization).

Change in the rotational axes (degree)	R_{wp}	***gof***
0	8.303	2.487
+ (plus)		
0.1x	8.306	2.487
0.2x	8.314	2.487
0.1y	8.306	2.487
0.2y	8.316	2.488
0.1z	8.305	2.487
0.2z	8.315	2.488
- (minus)		
0.1x	8.309	2.487
0.2x	8.316	2.488
0.1y	8.307	2.487
0.2y	8.317	2.488
0.1z	8.307	2.487
0.2z	8.318	2.488

Table S3(b). Impact on the R-factors over a manual shift in the translational axes of the DMF1 site Z-matrix (without further minimization).

Change in the translational axes (fractional unit)	***R_{wp}***	***gof***
0	8.303	2.487
+ (plus)		
0.01x	8.515	2.547
0.02x	9.153	2.738
0.01y	8.543	2.555
0.02y	9.250	2.767
0.01z	8.410	2.516
0.02z	8.726	2.610
- (minus)		
0.01x	8.537	2.553
0.02x	9.219	2.758
0.01y	8.536	2.553
0.02y	9.148	2.736
0.01z	8.396	2.511
0.02z	8.670	2.593

Table S3(c). Impact on the R-factors over a manual shift in the translational axes of the DMF1 site Z-matrix (***with*** further minimization).

Change in the translational axes (fractional unit)	***R_{wp}***	***gof***
0	8.303	2.487
+ (plus)		
0.1x+0.1y+0.1z	8.303	2.487
0.2x+0.2y+0.2z	9.498	2.841
- (minus)		
0.1x+0.1y+0.1z	9.946	2.975
0.2x+0.2y+0.2z	9.726	2.909

Table S4(a). Refinement evidence showing the preference of tetrahedral over octahedral coordination for Ag-ZSM-5 pre-adsorbed with DMF, by refining the SOF values of the water-ligand sites.

Species	Atom	*Refined SOF*	Species	Atom	*Refined SOF*
Z-matrix-Ag1	OAga1	0.2068	Z-matrix-Ag2	OAgb1	0.3483
	Aga	0.2068		Agb	0.3483
	OAga2	0.1192		OAgb2	0.3616
	OAga3	0.0029		OAgb3	0.0004
	OAga4	0.0000		OAgb4	0.0015
	OAga5	0.2698		OAgb5	0.3814
	OAgaf	0.2068		OAgbf	0.3483
	Ca2	0.2068		Cb2	0.3483
	Ca3	0.2068		Cb3	0.3483
	Ca4	0.2068		Cb4	0.3483
	Ca5	0.2068		Cb5	0.3483
	Ca6	0.2068		Cb6	0.3483
	Ca7	0.2068		Cb7	0.3483

Table S4(b). Refinement evidence showing the preference of tetrahedral over octahedral coordination for Cu-ZSM-5 pre-adsorbed with DMF, by refining the SOF values of the water-ligand sites.

Species	Atom	*Refined SOF*	Species	Atom	*Refined SOF*
Z-matrix-Cu1	OCua1	0.2334	Z-matrix-Cu2	OCub1	0.3744
	Cua	0.2334		Cub	0.3744
	OCua2	0.1811		OCub2	0.3476
	OCua3	0.0000		OCub3	0.0693
	OCua4	0.0000		OCub4	0.0305
	OCua5	0.2124		OCub5	0.4413
	OCuaf	0.2334		OCubf	0.3744
	Ca2	0.2334		Cb2	0.3744
	Ca3	0.2334		Cb3	0.3744
	Ca4	0.2334		Cb4	0.3744
	Ca5	0.2334		Cb5	0.3744
	Ca6	0.2334		Cb6	0.3744
	Ca7	0.2334		Cb7	0.3744

Table S4(c). Refinement evidence showing the preference of tetrahedral over octahedral coordination for Zn-ZSM-5 pre-adsorbed with DMF, by refining the SOF values of the water-ligand sites.

Species	Atom	*Refined SOF*	Species	Atom	*Refined SOF*
Z-matrix-Zn1	OZna1	0.1719	Z-matrix-Zn2	OZnb1	0.2793
	Zna	0.1719		Znb	0.2793
	OZna2	0.1531		OZnb2	0.2079
	OZna3	0.0003		OZnb3	0.0514
	OZna4	0.0003		OZnb4	0.0353
	OZna5	0.2131		OZnb5	0.1876
	OZnaf	0.1719		OZnbf	0.2793
	Ca2	0.1719		Cb2	0.2793
	Ca3	0.1719		Cb3	0.2793
	Ca4	0.1719		Cb4	0.2793
	Ca5	0.1719		Cb5	0.2793
	Ca6	0.1719		Cb6	0.2793
	Ca7	0.1719		Cb7	0.2793

Adsorption Values

Adsorbed 1.01 furan and 0.95 dimethylfuran (DMF) molecules per BAS are reported over H-ZSM-5 in the manuscript. These values were obtained from the TG data, i.e., 69 and 82 mg $g_{H\text{-}ZSM\text{-}5}^{-1}$, respectively. The values were further converted into the unit of 'molecule per acid site' based on the number of BASs per unit cell based on the structural formula of the H-ZSM-5 ($H_{4.48}Al_{4.48}Si_{91.52}O_{192}$). They gave the corresponding values of 0.91 and 0.86 mmol per $g_{H\text{-}ZSM\text{-}5}$', respectively, which are within experimental error when compared with the density of 0.9 mmol BASs per $g_{H\text{-}ZSM\text{-}5}$ as determined in the work by Teixeira *et al.* (Ref 3 of the main manuscript).

The contents of adsorbed furan and DMF in H-USY, Ag- and Zn-ZSM-5 are also summarised in Table S5. Although a slightly larger discrepancy is shown in the Zn-ZSM-5 sample, comparable quantities of adsorbed furan and DMF were measured in H- and Ag-ZSM-5 based on the thermogravimetric analysis (TGA) results within experimental errors. This suggests that the adsorption behaviours of the Lewis basic probe molecules on the acidic sites are similar in nature.

In contrast, there were large discrepancy between the adsorption of furan and DMF on H-USY based on the TGA results. On the other hand, the quantity of BASs of the H-USY (product ID = 360HUA) after heat treatment is 0.1 mmol g^{-1} as determined by NH_3-TPD given by TOSOH (the manufacturer of the H-USY). The notable difference between the quantity of the BASs and adsorbates (furan: 0.82 mmol g^{-1} and DMF: 1.49 mmol g^{-1}) is likely due to the formation organic cluster structures within the spacious void of H-USY generated by heat treatment in steam. Indeed, more organic like DMF can form extensive cluster structures in the gaseous and liquid phases based on computation calculations[9,10], where furan cluster aggregates are linked together *via* H-bonding interactions. The internal void space of H-USY is much larger than that in H-ZSM-5 (*cf*. 11.9 vs 7.0 Å), which can offer a much greater spatial freedom to facilitate the formation of such organic clusters. It infers that a large proportion of these aggregates can be located closer to the central space of the spherical void. The extra presence of the electron density in the centre of the void has been accounted by various 'dummy' atoms as described in the Method.

Table S5. The content of adsorbed furan and DMF in the zeolite samples.

Sample	Furan (mg g_{sample}^{-1})	DMF (mg g_{sample}^{-1})	Furan (mmol g_{sample}^{-1})	DMF (mmol g_{sample}^{-1})
H-USY	56	143	0.82	1.49
H-ZSM-5	69	82	0.91	0.86
Ag-ZSM-5	58	73	0.85	0.76
Zn-ZSM-5	46	84	0.67	0.87

Acknowledgements

The authors wish to thank the Hong Kong University Grants Committee (Early Career Scheme, Grant number: 25300918) for financial support of this collaborative work. We also acknowledge Beamline I11 at Diamond Light Source and Beamline BL02B2 at SPring-8 (Proposal number: 2018B1081) to offer beamtime.

References

1 B. T. W. Lo, L. Ye, J. Qu, J. Sun, J. Zheng, D. Kong, C. A. Murray, C. C. Tang and S. C. E. Tsang, *Angew. Chemie - Int. Ed.*, 2016, **55**, 5981–5984.

2 L. Ye, I. F. Teixeira, B. T. W. Lo, P. Zhao, S. C. Edman Tsang and E. Tsang, *Chem. Commun.*, 2017, **53**, 9725–9728.

3 S. P. Thompson, J. E. Parker, J. Marchal, J. Potter, A. Birt, F. Yuan, R. D. Fearn, A. R. Lennie, S. R. Street and C. C. Tang, *J. Synchrotron Radiat.*, 2011, **18**, 637–648.

4 N. H. Heo, C. W. Kim, H. J. Kwon, G. H. Kim, S. H. Kim, S. B. Hong and K. Seff, *J. Phys. Chem. C*, 2009, **113**, 19937–19956.

5 P. Thompson, D. E. Cox and J. B. Hastings, *J. Appl. Crystallogr.*, 1987, **20**, 79–83.

6 D. Watkin, *Acta Crystallogr. Sect. B Struct. Sci.*, 2000, **56**, 747–749.

7 R. I. Cooper, A. L. Thompson and D. J. Watkin, *J. Appl. Crystallogr.*, 2010, **43**, 1100–1107.

8 H. Van Koningsveld, *Acta Crystallogr. Sect. B Struct. Sci.*, 1990, **46**, 731–735.

9 B. F. Mentzen, *Mater. Res. Bull.*, 1987, **22**, 489–496.

10 R. Goyal, A. N. Fitch and H. Jobic, *J. Phys. Chem. B*, 2000, **104**, 2878–2884.